

Mathematical Model of the Population Dynamics of Brood Parasitism: What is the Benefit for the Host?

YOSHIHIRO HARAGUCHI AND HIROMI SENO†

Department of Biology, Faculty of Science, Kyushu University, Hakozaki 6-10-1, Higashi-ku, Fukuoka 812, Japan and Department of Mathematics, Faculty of Science, Hiroshima University, Kagamiyama 1-3-1, Higashi-hiroshima, Hiroshima 724, Japan

(Received on 18 April 1994, Accepted in revised form on 29 November 1994)

The problem of how the system of a brood-parasite with parasite-accepting host (i.e. a host that accepts a parasite's eggs) exists in stable equilibrium, is considered. We analyse a mathematical model of host-parasite population dynamics for this system, corresponding to certain cases of brood-parasitic animals where brood-parasitization causes drastic failure of the reproduction of the brood-parasitized host, and discuss the possible benefit to the persistence of a parasite-accepting host from the viewpoint of population dynamics.

1. Introduction

Brood-parasitism is a particular host-parasite relationship that has attracted a good deal of research in the ecological sciences (for an overview, see Krebs and Davies, 1987). It has been observed for a variety of birds (e.g. Rothstein, 1975*a, b*, 1982), insects (e.g. Hölldobler, 1971), and mochokid catfish in Lake Tanganyica, *Synodontis multipunctatus* (Sato, 1986, 1988). From an evolutionary viewpoint, the problem of why a brood-parasite with parasite-accepting host coexist stably is an interesting one. Rothstein (1982) suggested that the host simply lacks the ability to discriminate against the parasite's eggs, although once rejector genes appear in host population, they immediately spread. On the other hand, Dawkins & Krebs (1979) and Slatkin & Maynard Smith (1979) presented some alternative hypotheses on this problem:

(a) the parasite is sufficiently prudent to avoid over-exploiting the host population to extinction;

(b) all other host-parasite systems are unstable and have already gone extinct, so that we observe only stable ones;

(c) the host is one step ahead in the arms race against the parasite, driven by the *life-dinner principle*.

For a decreasing parasite population, the selection pressure on the host for further improvement becomes less and less. However, if a species of host population density becomes low, the parasite switches its preference for the host species to another, more abundant species. These hypotheses have been considered and examined in all observed brood-parasitisms. Various theoretical models have considered this problem. Takasu *et al.* (1993) analysed a mathematical model on the spread of rejector gene population with the assumption of rejection cost and showed the existence of the feasible evolutionarily stable state with an intermediate ratio of rejector gene population and that without rejector gene population. Nee & May (1993) discussed the possible relation between the evolutionary stability and the population dynamical stability of intra-specific brood-parasitism, making use of mathematical models. They stressed that the optimality and the evolutionarily stable strategy (ESS) of host and parasite strategies make

† Present address and address for correspondence: Department of Information and Computer Sciences, Nara Women's University, Kita-Uoya Nishimachi, Nara 630, Japan. Email: seno@ics.nara-wu.ac.jp.

sense only when the population dynamical equilibrium is stable. May & Robinson (1985) considered a mathematical model of the Nicholson–Bailey host–parasite system, and discussed the impact of brood-parasitism on host population persistence. They also considered the stability of equilibrium.

In case of the brood-parasitic mochokid catfish *Synodontis multipunctatus* in Lake Tanganyica, which can be regarded as an environment sufficiently stable over a long period, the catfish spawns its eggs into the eggs of its host, the mouth-brooder cichlid fish; for example, *Simochromis diagramma*. The catfish can reproduce only by brood-parasitism. In this case, no rejection by the host of brood-parasitization has yet been observed, so that it is likely that the host might completely accept the parasite's eggs. The parasite's eggs hatch before those of the host, and the juvenile parasites are reared in the host's mouth, using the host's eggs or juvenile hosts as their food (Sato, 1986, 1988). The safety level of mouth-brooding is very high for juveniles, so that brood-parasitism causes major mortality in juvenile hosts (i.e. drastic failure of reproduction in the brood-parasitized host) and results in a high survival rate for juvenile parasites in the parental care period.

Similar situations have also been observed in case of the brood-parasitic cuckoo, where the host's young are killed or the host's eggs are ejected from the nest (Krebs & Davies, 1987). For instance, the hedge warbler (dunnock) *Prunella modularis* has been observed as a parasite-accepting host for the cuckoo *Cuculus canorus* (Brooke & Davies, 1988). In the brood-parasitic brown-headed cowbird *Molothrus ater*, many host species are observed to be parasite acceptors (Rothstein, 1975a, b; 1982).

In such cases, where the host–parasite relationship is kept stationary, how does such a system keep its stability? Although the host appears to pay a high cost, there might be some possible benefits for it, or such a system might be stable in either an evolutionary or population-dynamical sense.

In this paper, we analyse a mathematical model of host–parasite population dynamics for brood-parasitism with a parasite-accepting host, in particular referring to the case of the mochokid catfish, *Synodontis multipunctatus*. We discuss the possible benefit for the host from the standpoint of population-dynamical stability, rather than from the evolutionary viewpoint of other theoretical studies. In contrast to the mathematical considerations by May & Robinson (1985) and Nee and May (1993), we focus on the lowest host population density at the stationary

state and include not only equilibrium but also periodic and chaotic states. We consider that it would be more beneficial for the persistence of the host population if the lowest population density at the stationary state is higher, because the generation with the lower lowest density can be regarded as relatively more vulnerable to stochastic disturbance, which might drastically damage the persistence of host population. The host–parasite system can be maintained only when the persistence of host population is sufficiently high. We discuss how the persistence of the parasite-accepting host population depends on coexistence with the brood-parasite, compared to the case where the host population exists without the brood-parasite. In this sense, our work is related close to the second hypothesis (b) mentioned above. We also discuss hypothesis (a) in the framework of our mathematical model.

2. Model

2.1. MODELLING ASSUMPTION

Since our interest is in the population-dynamical nature of a stationarily persisting host–parasite system, we do not consider any evolutionary exchange of species (i.e. the process in which the evolutionarily dominant parasite species succeeds in the invasion and sweeps away the evolutionarily subordinate parasite species that previously coexisted with the host). Hence, the considered parasite may be regarded as one with an evolutionarily stable strategy (ESS), so that the host–parasite system is either a highly coevolved one, or persists for a long period of evolutionary history before any evolutionary change. Thus we assume that there is no phenotypic variation in both host and parasite populations.

Each generation is assumed to be composed of three distinct periods: brood-parasitization period; parental care period; and fertilization period (Fig. 1).

Brood-parasitization period

This corresponds to the breeding season for parasite and host. In this period, brood-parasitization by adult parasite occurs for adult host. As in case of *Synodontis multipunctatus* in Lake Tanganyica, the host completely accepts the brood-parasitization without any sign of rejecting the parasite's eggs. Adult hosts consist of brood-parasitized and non-parasitized individuals. The brood-parasite is assumed to reproduce only by brood-parasitization. The expected number of brood-parasite's eggs can be estimated from the brood-parasitized adult host population.

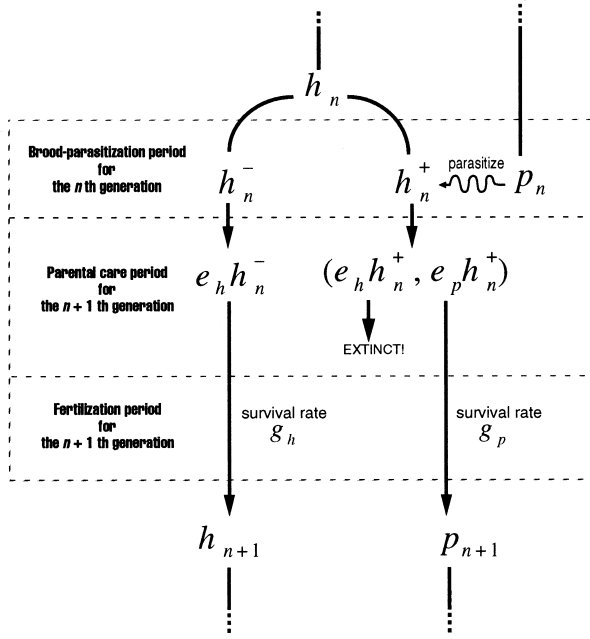


FIG. 1. Brood-parasitism composed of three distinct periods: brood-parasitization period, parental care period, and fertilization period. For detailed explanation, see text.

Parental care period

The adult brood-parasite excludes all of host's eggs, or the juvenile parasites kill or exclude all of host's eggs or juvenile hosts after hatching, as in case of *Synodontis multipunctatus*. In the latter case, at the beginning of this period, the host has both its own and parasite's eggs together. However, both the host's eggs and juvenile hosts with brood-parasitized adult host go extinct in this period. The brood-parasitized host's parental care provides juvenile parasites with a high survival rate in this period—by mouth-brooding the brood-parasitized host cichlid fish in the case of *Synodontis multipunctatus*.

Fertilization period

At the beginning of this period, adults and juveniles coexist independently of each other. However, for simplicity, it is assumed that both adult hosts and parasites of the previous generation go extinct, or become a small enough population (compared to that of growing juveniles) to be neglected, before their juveniles grow up to reproductive adults (*non-overlapping generation*). Therefore, expected adult host and parasite population densities in the breeding season at each generation, just after the fertilization period, are determined only by the survival rate of juvenile populations through this period.

2.2. GENERAL SYSTEM

Let \$h_n\$ denote adult host population density at the \$n\$-th generation, and \$h_n^+\$ and \$h_n^-\$ population density of brood-parasitized and non-parasitized adult host, respectively, at the \$n\$-th generation. Then, the relation among \$h_n\$, \$h_n^+\$ and \$h_n^-\$ is given by

$$h_n = h_n^+ + h_n^- \tag{1}$$

Adult host population density at the \$(n+1)\$-th generation is assumed to depend only on the juvenile population density of non-parasitized adult host at the \$n\$-th generation, because the reproduction of the brood-parasitized adult host is now assumed to fail completely. In our model, adult host population density \$h_{n+1}\$ and adult parasite population density \$p_{n+1}\$ at the \$(n+1)\$-th generation are as follows:

$$h_{n+1} = e_h h_n^- g_h(e_h h_n^-) \tag{2}$$

$$p_{n+1} = e_p h_n^+ g_p(e_p h_n^+), \tag{3}$$

where \$e_h\$ and \$e_p\$ are the intrinsic reproduction rates per unit adult density for host and parasite respectively (see Fig. 1). So \$e_h h_n^-\$ and \$e_p h_n^+\$ correspond respectively to juvenile host and juvenile parasite population density just after the parental care period for the \$(n+1)\$-th generation. \$g_i\$ (\$i=h, p\$) introduces the survival rate function through the fertilization period for juveniles to grow up to adults reproductive in the breeding season, such that

$$0 \leq g_i(x) \leq 1 \quad (i=h, p). \tag{4}$$

On the other hand, the brood-parasitized adult host population density at the \$n\$-th generation is given by

$$h_n^+ = f(p_n) h_n, \tag{5}$$

where \$f(x)\$ gives the parasitization rate per adult host density when adult parasite population density is \$x\$. It is assumed to satisfy the following natures:

$$0 \leq f(x) \leq 1 \tag{6}$$

$$f(0) = 0 \tag{7}$$

$$\frac{df(x)}{dx} \geq 0. \tag{8}$$

Equation (7) means that parasitization does not occur without parasite. Equation (8) shows that large parasite population density causes a high parasitization rate. Now, from (1) and (5), non-parasitized adult host population density \$h_n^-\$ can be expressed as follows:

$$h_n^- = [1 - f(p_n)] h_n. \tag{9}$$

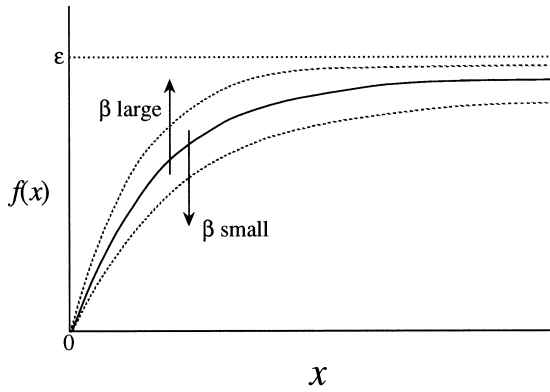


FIG. 2. Parasitization rate $f(x)$ for parasite density x , given by eqn (12). For larger β , $f(x)$ becomes higher.

Finally, from (5) and (9), the system of (2) and (3) can be described as

$$h_{n+1} = e_h [1 - f(p_n)] h_n g_h(e_h [1 - f(p_n)] h_n) \quad (10)$$

$$p_{n+1} = e_p f(p_n) h_n g_p(e_p f(p_n) h_n). \quad (11)$$

2.3. PARASITIZATION RATE FUNCTION

We consider the following type of increasing saturation function for the parasitization rate function f , which satisfies conditions (7), (6) and (8) (Fig. 2):

$$f(x) = \frac{\epsilon \beta x}{1 + \beta x} \quad (x \geq 0), \quad (12)$$

where ϵ is a positive constant ≤ 1 , which now corresponds to the upper bound of parasitization rate, and β is a positive weight constant. For a fixed finite value of β , as x increases, $f(x)$ monotonically approaches ϵ from the below. As $\beta \rightarrow \infty$, $f(x)$ becomes constant: $f(x) \rightarrow \epsilon$.

The relationship via parasitization between parasite and host depends on a variety of factors, including the behaviour of parasite and host, so that a proportion of host population can escape from parasitization even when parasite density is very high, and the parasitization rate can be always less than ϵ which is the upper bound determined by such factors.

The parasitization rate $f(x)$ for each parasite density x becomes large as the β becomes large. Hence, β can be regarded as related to the parasitization efficiency, which depends on the parasite's behaviour as its tactic for parasitization, for example.

2.4. LOGISTIC TYPE REPRODUCTION

We consider the following survival rate function g_i ($i = h, p$):

$$g_i(x) = \begin{cases} a_i \left(1 - \frac{x}{e_i c_i}\right) & \text{when } 0 \leq x \leq e_i c_i \\ 0 & \text{otherwise,} \end{cases} \quad (13)$$

where a_i and c_i ($i = h, p$) are positive constants and $0 < a_i < 1$. Parameter a_i corresponds to the intrinsic survival rate. In this model, the parameter value represented by $e_i c_i$ corresponds to the carrying capacity for *juvenile* hosts ($i = h$) or *juvenile* parasites ($i = p$). From (2) and (3), if juvenile population density, $e_h h_n^-$ or $e_p h_n^+$, just after the parental care period is respectively lower than and near to $e_h c_h$ or $e_p c_p$, the survival rate given by (13) becomes very small. This corresponds to the case when juvenile population decreases due to the shortage of resources or to the relatively high predation risk, or to some other environmental exhaustion because of the high juvenile population density at the beginning of fertilization period.

With (12) and (13), the system of (10) and (11) now becomes

$$h_{n+1} = a_h e_h \left(1 - \frac{\epsilon \beta p_n}{1 + \beta p_n}\right) \times h_n \left[1 - \left(1 - \frac{\epsilon \beta p_n}{1 + \beta p_n}\right) \frac{h_n}{c_h}\right] \quad (14)$$

$$p_{n+1} = a_p e_p \frac{\epsilon \beta p_n}{1 + \beta p_n} h_n \left(1 - \frac{\epsilon \beta p_n}{1 + \beta p_n} \frac{h_n}{c_p}\right). \quad (15)$$

This system has a specific nature regarding the reproduction of parasite and host, which we now call *logistic type*: both (14) and (15) have the nature of a unimodal map, as shown in Fig. 3. In particular, when $p_n \equiv 0$, that is, when the parasite is absent, the system of (14) and (15) becomes one-dimensional:

$$h_{n+1} = a_h e_h h_n \left(1 - \frac{h_n}{c_h}\right). \quad (16)$$

This corresponds to the well-known discrete logistic dynamical system studied by May (1976) and other mathematical researchers (for instance, Baker & Gollub, 1990). This system can provide a variety of stationary states for the host population with the absence of parasite, depending on the parameters, to which we will return later. Such a variety of stationary states have also been discussed for real populations or in experiment, for example, by Utida (1957) (see also Chapter 6 in Begon *et al.*, 1990).

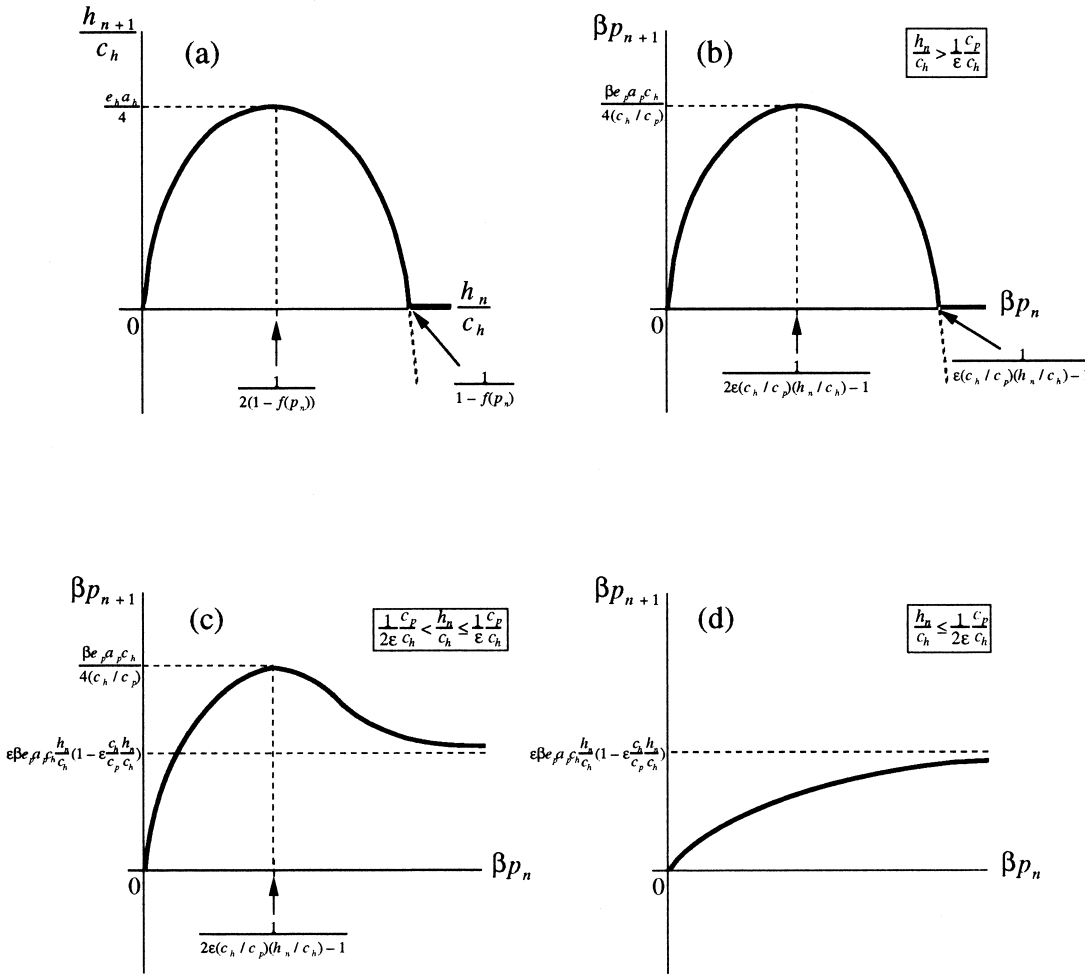


FIG. 3. (a) Map $h_n/c_h \rightarrow h_{n+1}/c_h$ corresponding to eqn (14). When $h_n/c_h \geq 1/(1-f(p_n))$, $h_{n+1} \equiv 0$. (b) Map $\beta p_n \rightarrow \beta p_{n+1}$ corresponding to (15) when $h_n > c_p/\epsilon$. When $\beta p_n \geq c_p/(c_h - c_p)$, $p_{n+1} \equiv 0$. (c) Map $\beta p_n \rightarrow \beta p_{n+1}$ when $c_p/2\epsilon < h_n \leq c_p/\epsilon$. (d) Map $\beta p_n \rightarrow \beta p_{n+1}$ when $h_n < c_p/2\epsilon$.

2.5. NON-DIMENSIONALIZED VARIABLE SYSTEM

With some appropriate non-dimensionalized variables, the system of (14) and (15) can be expressed in the mathematically equivalent form:

$$H_{n+1} = A_H [1 - \epsilon F(P_n)] H_n \{1 - [1 - \epsilon F(P_n)] H_n\} \tag{17}$$

$$P_{n+1} = \epsilon A_P F(P_n) H_n \{1 - \epsilon B_P F(P_n) H_n\}, \tag{18}$$

where

$$\begin{aligned} H_i &\equiv \frac{h_i}{c_h} \\ P_i &\equiv \beta p_i \\ A_H &\equiv e_h a_h \\ A_P &\equiv \beta e_p a_p c_h \end{aligned}$$

$$B_P \equiv \frac{c_h}{c_p}$$

$$F(x) \equiv \frac{x}{1+x}.$$

2.6. INITIAL STATE

Since $e_h c_h$ means the carrying capacity for juvenile host population so that $h_i/c_h = e_h h_i / e_h c_h < 1$ for meaningful positive h_i , the corresponding non-dimensionalized variable H_i can be meaningfully considered less than 1. Hence, we consider the initial H_0 less than 1.

As for the initial P_0 , we consider only a sufficiently small value. This is because our interest is in the stationary state approached after a large number of generations, and it is regarded as biologically natural to consider the initial parasite to be at the stage

of *invasion*. Coexistence between parasite and host requires the parasite to invade successfully at the first stage.

2.7. MODELLING CONSTRAINT FOR PARAMETERS

For well-defined behaviour as a biological model, our system should be considered under the mathematical constraint for parameters below, which assures that (H_n, P_n) are non-negative for any $n \geq 1$ and for any non-negative initial condition (H_0, P_0) satisfying the condition given in the previous section (see Appendix A):

$$0 \leq A_H \leq \min \left\{ 4, \frac{4}{\epsilon} \left(\frac{4}{A_P} + \frac{1}{B_P} \right) \right\}. \tag{19}$$

Unless parameters satisfy this *confinement condition*, there exist such some initial values (H_0, P_0) that H_n or P_n becomes negative at some n .

2.8. PARAMETERS FOR *SYNODONTIS MULTIPUNCTATUS*

Some, but not all, parameters of our model can be estimated from observed data. In case of the brood-parasitism of *Synodontis multipunctatus*, with host mouth-brooder cichlid fish, Sato (1986, 1988) reported that the parasitization rate ranges from 1.4% to 15.0%, and is 6.3% on average. In our model, the parasitization rate is given by the function of host population density. Thus, following observations by Sato (1986, 1988), we could, for example, set the upper bound ϵ of the parasitization rate as 0.1, that is, 10.0%.

On the other hand, from Sato's observations, the host mouth-brooder cichlid fish keeps about 20 eggs on average per individual, and the number of brood-parasite catfish eggs in the host mouth is about three on average per parasitized host individual. These data can be considered to correspond to parameters e_h and e_p in our model. Since both juvenile cichlid fish and juvenile catfish commonly feed benthos in the mouth-brooding period, that is, in the parental care period in our model, we assume that they would share a common niche, so that they have the same carrying capacity. This corresponds to the following relation among parameters in our model: $e_h c_h \sim e_p c_p$. With this supposition, we can estimate the value of parameter B_P in this case from the definition:

$$B_P \equiv \frac{c_h}{c_p} = \frac{e_p}{e_h} \cdot \frac{e_h c_h}{e_p c_p} \sim \frac{e_p}{e_h} \sim \frac{3}{20} = 0.15.$$

We remark that, with the assumption of common carrying capacity between juvenile hosts and parasites, the value of parameter B_P is, in general, < 1 , because the number of parasite eggs e_p parasitized by adult parasite is usually less than the number of host eggs e_h with them, which can be observed for a variety of brood-parasitisms. For the case corresponding to an observed brood-parasitism, we assume that $\epsilon = 0.1$ and $B_P = 0.15$.

3. Analysis

3.1. EQUILIBRIUM STATE AND ITS LOCAL STABILITY

In this section, we consider the equilibrium state (H^*, P^*) for the system of (17) and (18), which satisfies the following:

$$\begin{cases} H^* \{ 1 - A_H [1 - \epsilon F(P^*)] (1 - [1 - \epsilon F(P^*)] H^*) \} = 0 \\ P^* - \epsilon A_P F(P^*) H^* \{ 1 - \epsilon B_P F(P^*) H^* \} = 0. \end{cases} \tag{20}$$

One equilibrium state is such that both parasite and host completely die out: $(H^*, P^*) = (0, 0)$ (Case 1). Another is such that host persists and parasite goes extinct: $(H^*, P^*) = (+, 0)$ (Case 2). In the latter case, since $F(0) = 0$, H^* is given from (20) by

$$H^* = 1 - \frac{1}{A_H}. \tag{21}$$

In the case when parasite and host coexist: $(H^*, P^*) = (+, +)$ (Case 3), we must look for the positive (H^*, P^*) which satisfies both conditions of (20). Number of possible solutions for (H^*, P^*) significantly depends on parameters. For any parameters which satisfy the confinement condition (19), making use of a number of numerical calculations, only one meaningful positive solution (H^*, P^*) for (20) can be found (see Appendix B).

For Case 1 when $(H^*, P^*) = (0, 0)$, and for Case 2 when $(H^*, P) = (+, 0)$, the following conditions can be analytically obtained for the local stability (Appendix C):

Case 1: $(H^*, P^*) = (0, 0)$:

$$0 < A_H < 1. \tag{22}$$

Case 2: $(H^*, P^*) = (+, 0)$:

$$\max \left\{ \frac{1}{3}, 1 - \frac{1}{\epsilon A_P} \right\} < \frac{1}{A_H} < 1. \tag{23}$$

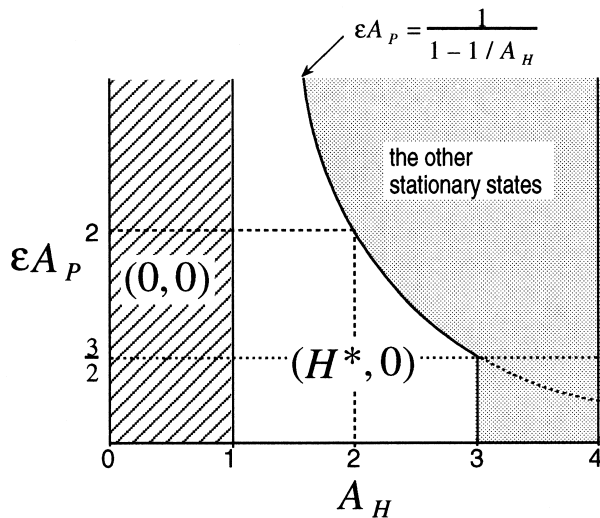


FIG. 4. Parameter regions of the local stability for $(H^*, P^*) = (0, 0)$ and for $(H^*, P^*) = (+, 0)$.

As indicated in Fig. 4, the stability of the equilibrium state $(H^*, P^*) = (+, 0)$ becomes less as the value of ϵA_P gets larger. The stability of the equilibrium state $(H^*, P^*) = (0, 0)$ is independent of both ϵ and A_P . Thus a parasite with a large value of ϵA_P could possibly be more successful in its invasion and coexistence with a host with $A_H > 1$. This result will be more clearly shown by the analysis carried out in the next section.

In Case 3, since the equilibrium state $(H^*, P^*) = (+, +)$ could not be obtained in any practical form, we examined local stability by numerical calculations only. Numerical calculations show that the resulting local stability for these equi-

librium states (H^*, P^*) of three cases coincide with their global stability, which will be shown in the next section. The result for the parameter region for the stability for Case 3, is given in the next section.

3.2. BIFURCATION STRUCTURE

Case without parasite ($P_n \equiv 0$)

As already mentioned for (16), this corresponds to the case of the well-known one-dimensional system studied by May (1976) and other researchers. As the parameter A_H increases, the *pitch-fork bifurcation* to chaos takes place, as shown in Fig. 5(a): The stable stationary state subsequently changes from the equilibrium (i.e. 1-periodic) to 2-periodic at $A_H = 3.0$, then to 4-periodic, to 8-periodic, etc., in a *period-doubling* manner (as for this type of bifurcation, for instance, see Devaney, 1989). For A_H larger than 3.569..., the chaotic stationary state appears with an infinite number of windows of the other periodic stationary states.

In Fig. 5(b), the mean and the lowest host population densities at the stable stationary state in this case are shown numerically. For the parameters region corresponding to the equilibrium state, the case where both the mean and the lowest densities coincide with the equilibrium value of H^* itself is trivial. As indicated in Fig. 5(b), the lowest density takes its maximum at $A_H = 3$ and is monotonically decreasing as $A_H > 3$ increases. In contrast, the mean density seems to tend to decrease as $A_H > 3$ increases, though it shows some complex behaviour in detail for the parameter region corresponding to the chaotic state.

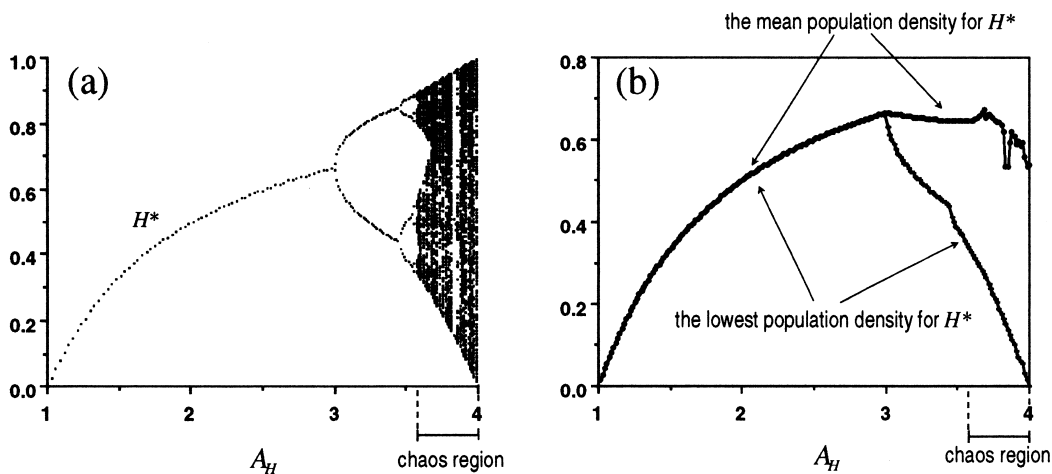


FIG. 5. (a) Bifurcation structure for the stable stationary state in the case when parasite is absent ($P^* \equiv 0$). Population density H^* at the stationary state is plotted. (b) Plots of the lowest and the mean host population densities at the stationary state in the case when parasite is absent.

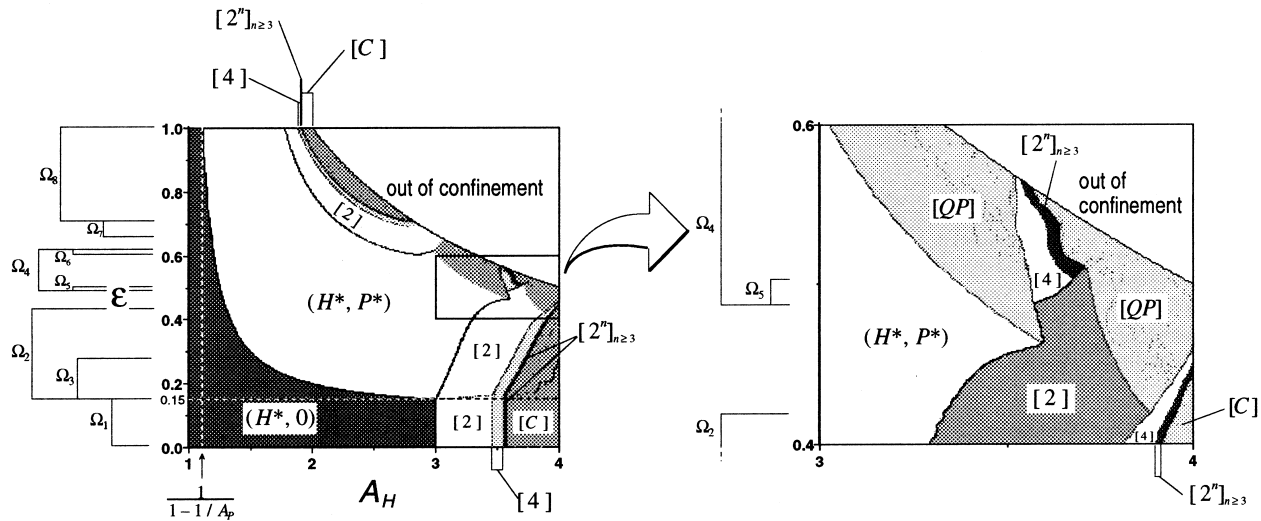


FIG. 6. (A_H, ϵ) -dependence of the stable stationary state, obtained by numerical calculations. $H_0 = P_0 = 0.1$; $A_p = B_p = 10.0$. Terms in brackets [] express the period of the stable periodic state for the corresponding parameter region. Exceptionally, $[2^n]_{n \geq 3}$ corresponds to the region where period-doubling from 2^j to 2^∞ as A_H increases for fixed ϵ . [C] corresponds to the region for the chaotic state with an infinite number of windows of the other periodic states, and [QP] does that for the stable quasi-periodic state. For $A_H < 1$, both parasite and host go extinct. For regions Ω_i of ϵ , see text.

Case with brood-parasite

In case of two-species system, the bifurcation involves complex structure. In Fig. 6, the complex structure is exemplified, with numerical calculations for $A_p = B_p = 10.0$. The result on the stability of equilibrium state perfectly coincides with that of the local stability analysis carried out in the previous section.

When ϵ is of the region Ω_1 shown in Fig. 6, the bifurcation structure of stable stationary state

coincides with that when the parasite is absent, because the parasite eventually goes extinct (as indicated in Fig. 7). For some ϵ of the region Ω_2 in Fig. 6, in contrast, parasite and host can coexist (Fig. 7) and every bifurcation point then appears to shift relatively to the right-hand side, that is, to the side for the larger value of A_H . The bifurcation is lead to chaos as A_H increases (Fig. 8). In particular, as shown in Fig. 7 and Fig. 9, for ϵ in the Ω_3 subregion of Ω_2 , parasite and host coexist only for some intermediate range of A_H , while parasite goes extinct for sufficiently small or large A_H .

Our two-species system has the potential to show other types of bifurcation. For instance, as A_H increases with fixed ϵ in the Ω_4 region in Fig. 6, the equilibrium state becomes unstable and the orbit is attracted to a closed curve in the phase space (H_n, P_n) (see Figs 10 and 11). This is known as a *Naimark–Sacker bifurcation*. If the initial point is on the closed curve, the orbit densely wanders on the whole curve (or some parts of it) without returning to the same point. This type of stationary state in which the orbit is wandering on a closed curve can be called *quasi-periodic* (for instance, see Wiggins, 1990).

Further, the *backward pitch-fork bifurcation* can appear. For one example, as A_H increases with fixed ϵ in the Ω_5 region in Fig. 6, the stationary state changes from a quasi-periodic state to 4-periodic one, and subsequently to 2-periodic (see Fig. 10). For another example, as A_H increases with fixed ϵ in the Ω_6 region in Fig. 6, the equilibrium state changes to

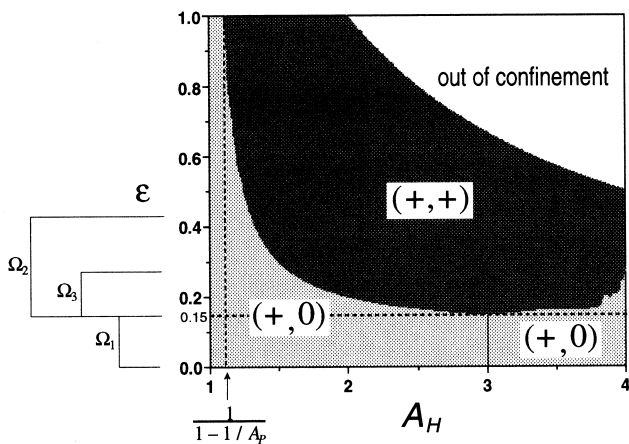


Fig. 7. (A_H, ϵ) -dependence of the coexistence between host and parasite, obtained by numerical calculations. The region $(+, 0)$ corresponds to where host persists while parasite goes extinct. The region $(+, +)$ corresponds to coexistence host and parasite. For $A_H < 1$, both parasite and host go extinct.

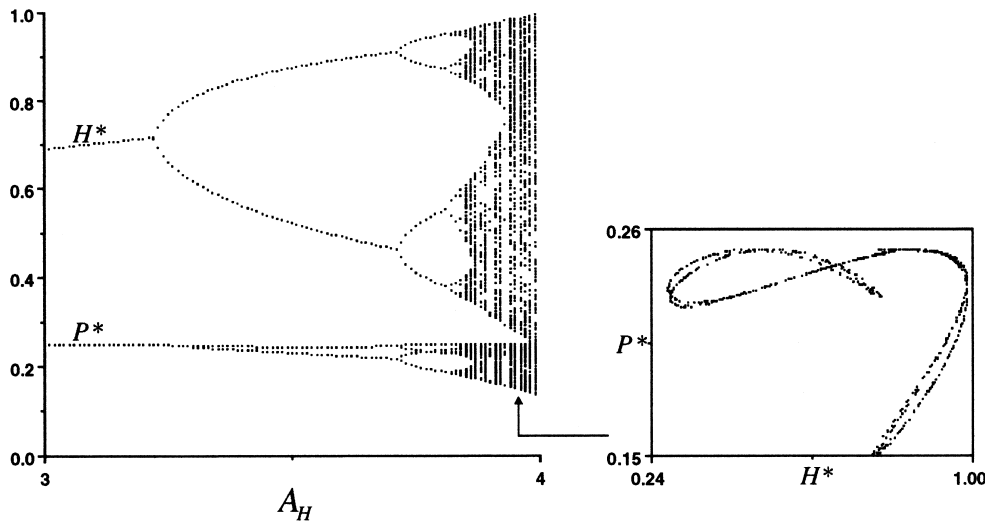


FIG. 8. Bifurcation of the stable stationary state for Ω_2 in Fig. 6. $H_0 = P_0 = 0.1$; $A_p = B_p = 10.0$; $\epsilon = 0.35$; $2.0 \leq A_H \leq 4.0$. Population densities H^* and P^* at the stationary state are plotted. The orbit of (H^*, P^*) in the phase space is also shown for $\epsilon = 0.35$ and $A_H = 3.95$.

2-periodic and again returns to the equilibrium state (Fig. 11).

For ϵ in the Ω_8 region in Fig. 6, another pitch-fork bifurcation structure exists. In the chaotic state approached from the pitch-fork bifurcation, the attractor appears similar to a Hénon attractor, as seen in Fig. 12 (Hénon, 1976).

On the other hand, under the confinement condition (19), the case exists where the system does not show

bifurcation to chaos as A_H increases. With fixed ϵ in Ω_7 in Fig. 6, the bifurcation under consideration consists of only a period-doubling structure with finite periods (Fig. 13).

In spite of the potential of these complex bifurcation structures for $A_p = B_p = 10.0$, numerical calculations for the case when $\epsilon = 0.1$ and $B_p = 0.15$ show simpler bifurcation structures as seen in Fig. 14. It seems very similar to the bifurcation structure for the Ω_1 and Ω_2 regions in Fig. 6 for the case when $A_p = B_p = 10.0$. As shown in Figs 14 and 15, when parasite and host coexist, compared to when parasite goes extinct, every bifurcation point shifts relatively to the right-hand side, that is, to the side with the larger value of A_H . Numerical calculations show that the bifurcation points monotonically shift as A_p increases, and no other bifurcation structure appears in this case. Therefore, in this case, if parasite succeeds to invade and coexist with host, which would be in q_0 -periodic stationary state without parasite, the coexistent stationary state appears q_+ -periodic such that $q_+ \leq q_0$. In particular, the generationally chaotic variation of host population density without parasite could disappear and stabilize to some periodic stationary state by coexistence with parasite. Coexistence between parasite and host might have the tendency to suppress the generational variation of host density, compared to the variation without parasite. This tendency will be more clearly explained in the analysis given in the next section.

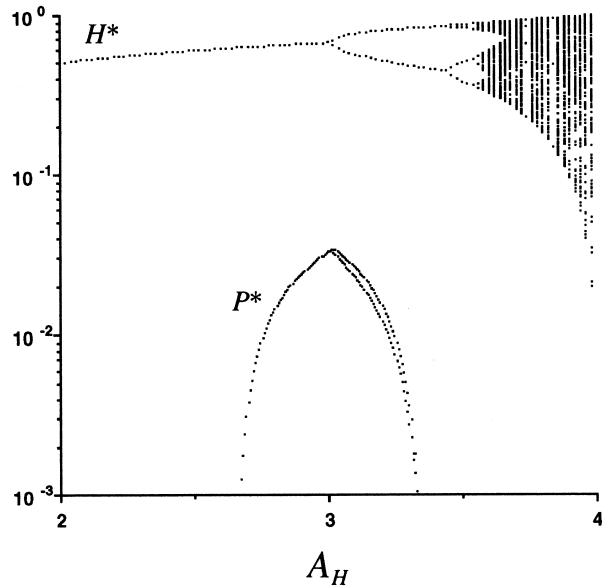


FIG. 9. Bifurcation of the stable stationary state for Ω_3 in Fig. 6. $H_0 = P_0 = 0.1$; $A_p = B_p = 10.0$; $\epsilon = 0.16$; $2.0 \leq A_H \leq 4.0$. Population densities H^* and P^* at the stationary state are plotted. Vertical axis is logarithmic.

In both cases, the result of the stability of the equilibrium state perfectly coincides with that of the local stability analysis carried out in the previous

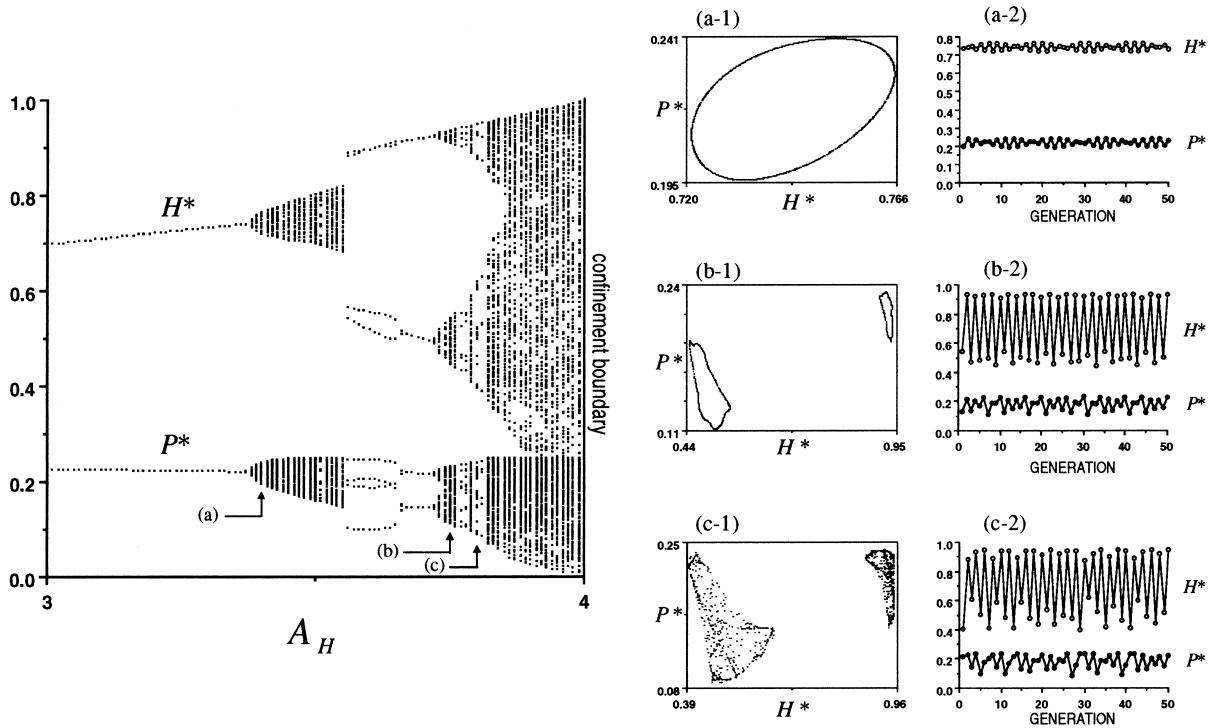


FIG. 10. Bifurcation of the stable stationary state for Ω_5 in Fig. 6. $H_0 = P_0 = 0.1$; $A_p = B_p = 10.0$; $\epsilon = 0.5$; $3.0 \leq A_H \leq 4.0$. Population densities H^* and P^* at the stationary state are plotted. For some ranges of A_H , (H^*, P^*) so rapidly changes state that numerical results appear disconnected. Some orbits in the phase space and generational variations of (H^*, P^*) at the stationary state are shown: (a) $A_H = 3.4$; (b) $A_H = 3.75$; (c) $A_H = 3.8$.

section. As already mentioned in the local stability analysis, coexistence between parasite and host depends significantly on the value of ϵA_p . Indeed, the

parameter region for coexistence appears very similar between two cases considered by numerical calculations (compare Fig. 7 with Fig. 15). Also in the case

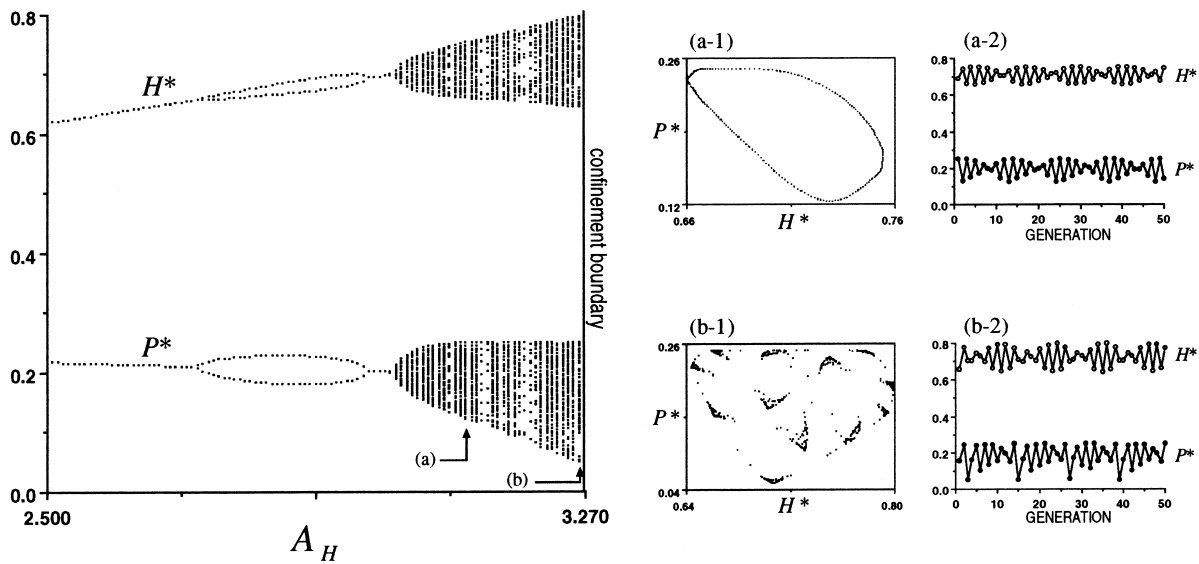


FIG. 11. Bifurcation of the stable stationary state for Ω_6 in Fig. 6. $H_0 = P_0 = 0.1$; $A_p = B_p = 10.0$; $\epsilon = 0.612$; $2.0 \leq A_H \leq 3.26797$. Population densities H^* and P^* at the stationary state are plotted. Some orbits in the phase space and generational variations of (H^*, P^*) at the stationary state are shown: (a) $A_H = 3.1$; (b) $A_H = 3.26$.

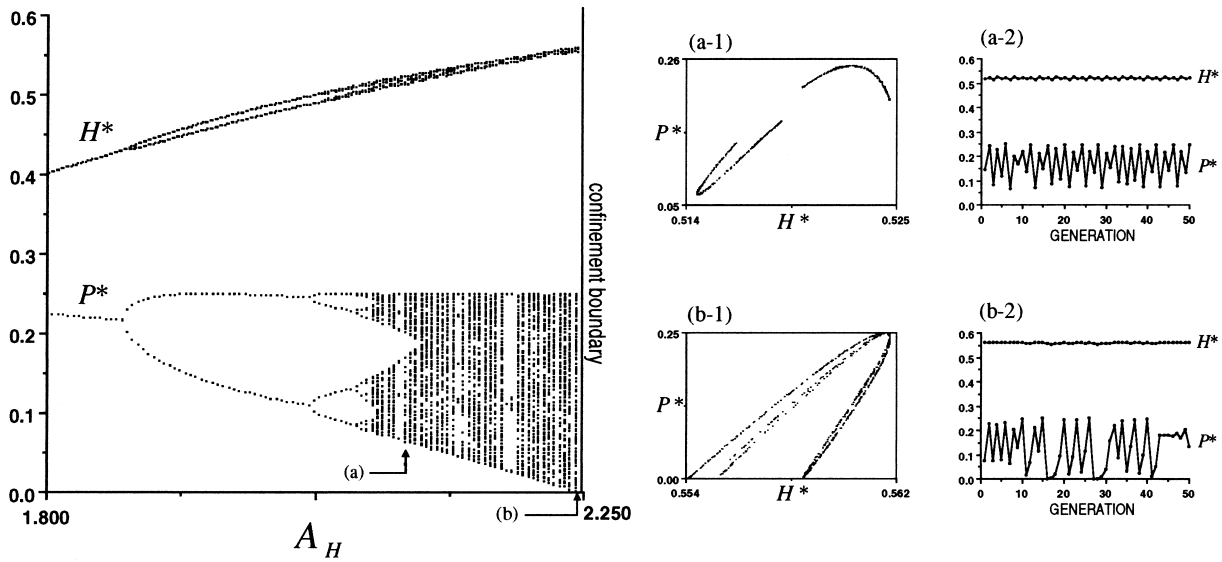


FIG. 12. Bifurcation of the stable stationary state of Ω_2 in Fig. 6. $H_0 = P_0 = 0.1$; $A_p = B_p = 10.0$; $\epsilon = 0.89$; $1.8 \leq A_H \leq 2.24719$. Population densities H^* and P^* at the stationary state are plotted. Some orbits in the phase space and generational variations of (H^*, P^*) at the stationary state are shown: (a) $A_H = 2.1$; (b) $A_H = 2.247$.

when $\epsilon = 0.1$ and $B_p = 0.15$, analogously to the case for the region Ω_3 in Fig. 6, there exists a parameter region of A_p such that parasite and host coexist only for some intermediate range of A_H , while parasite goes extinct for sufficiently small or large A_H (see Fig. 15). This result indicates that there exists an intermediate range for the value of ϵA_p such that parasite and host coexist only for the intermediate range of A_H , and parasite goes extinct for A_H out of the range. With ϵA_p below

the range, parasite goes extinct for any A_H , while, with ϵA_p beyond it, parasite and host coexists for any A_H greater than a certain threshold (see Fig. 7 and Fig. 15).

3.3. PARASITE-DEPENDENCE OF HOST POPULATION DENSITY

In this section, making use of numerical calculations, we compare the mean and the lowest host population densities at the stable stationary state when parasite and host coexist with those when the parasite is absent [see Fig. 5(b)]. The difference of these densities is naturally 0 between the two cases for parameters such that parasite eventually goes extinct: the corresponding parameter region is indicated as D_{00} in Fig. 16(a) for $A_p = B_p = 10.0$ and in Fig. 16(b) for $\epsilon = 0.1$ and $B_p = 0.15$, which coincides with the parameter region indicated by $(+, 0)$ in Figs 7 and 15. Our numerical calculations show the other parameter regions shown in Fig. 16, for which there are four cases.

- (i) Both the mean and the lowest densities are higher when parasite and host coexist than when parasite is absent, D_{++} ;
- (ii) the mean is larger while the lowest is smaller, D_{+-} ;
- (iii) the mean is smaller while the lowest is larger, D_{-+} ;
- (iv) both are smaller, D_{--} .

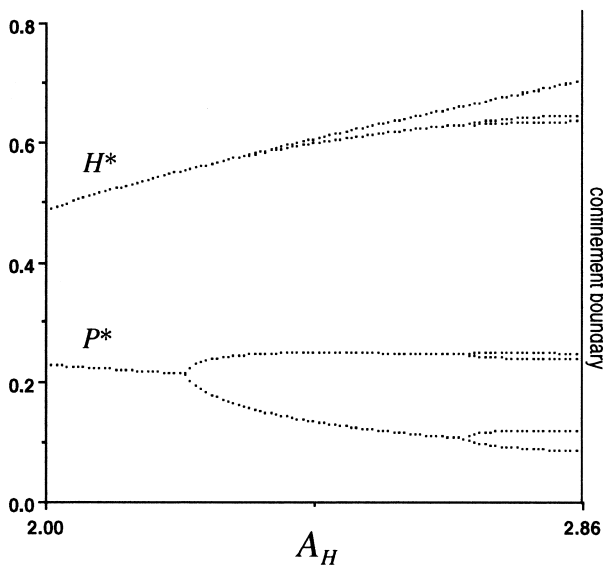


FIG. 13. Bifurcation structure at the stable stationary state for Ω_7 in Fig. 6. $H_0 = P_0 = 0.1$; $A_p = B_p = 10.0$; $\epsilon = 0.7$; $2.0 \leq A_H \leq 2.85714$. Population densities H^* and P^* at the stationary state are plotted.

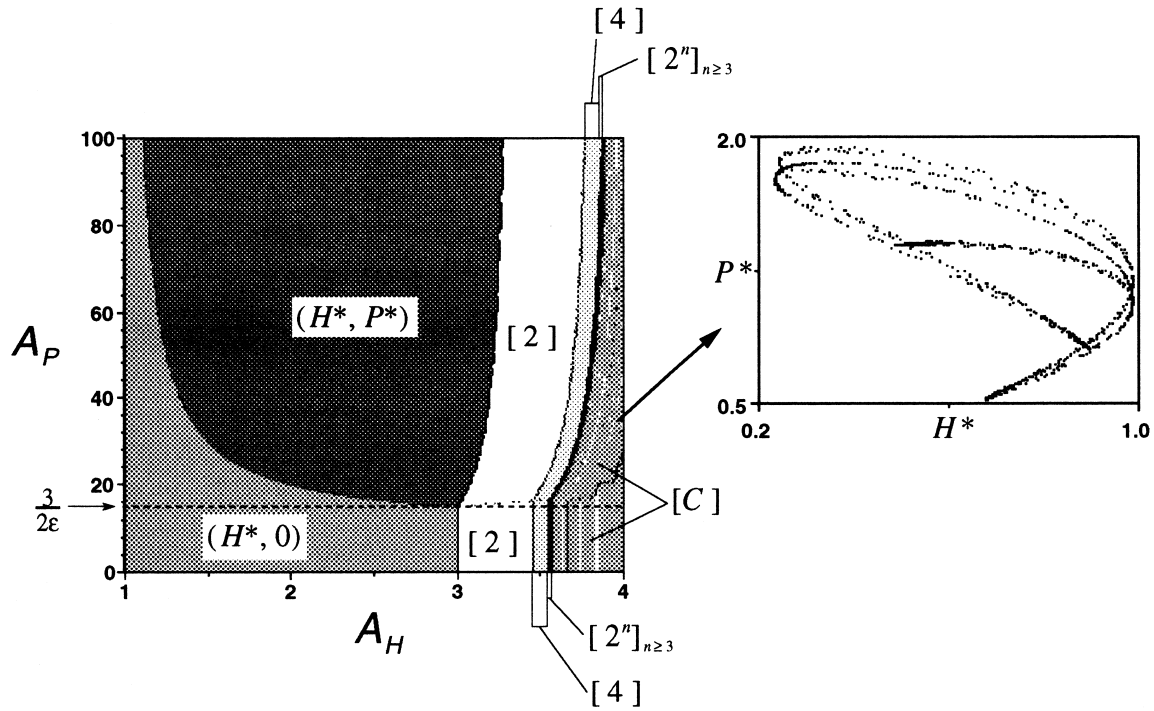


FIG. 14. (A_H, A_P) -dependence of the stable stationary state, obtained by numerical calculations. $H_0 = P_0 = 0.1$; $\epsilon = 0.1$; $B_P = 0.15$. Terms in brackets [] are as in Fig. 6. The orbit of (H^*, P^*) in the phase space is also numerically shown for $A_P = 35.0$ and $A_H = 3.95$.

We consider that it would be more beneficial for the persistence of host population if the lowest population density at the stationary state is higher, because the generation with the lower lowest density can be regarded as relatively more vulnerable for

stochastic disturbance, which might cause drastic damage to the persistence of host population. If the coexistence at the stationary state corresponds to the parameter region D_{++} or D_{-+} , coexistence can be regarded as beneficial for host from the viewpoint of population persistence. The host-parasite system can be maintained only when the persistence of host population is sufficiently high.

Parameter regions D_{+-} and D_{-+} are relatively small. Roughly speaking, parameter region D_{++} exists for large A_H , while D_{--} is for small A_H . The boundary between D_{--} and D_{++} in Fig. 16 can be analytically identified, as long as it is in the parameter region for equilibrium state (Appendix D):

$$\epsilon A_P = \frac{\epsilon}{1-\epsilon} \cdot \frac{1}{B_P+1} \cdot \frac{A_H^2}{\left(\frac{2-\epsilon}{1-\epsilon} - A_H\right)\left(A_H - \frac{2B_P}{B_P+1}\right)}, \quad (24)$$

where

$$2 < A_H < \frac{2-\epsilon}{1-\epsilon}. \quad (25)$$

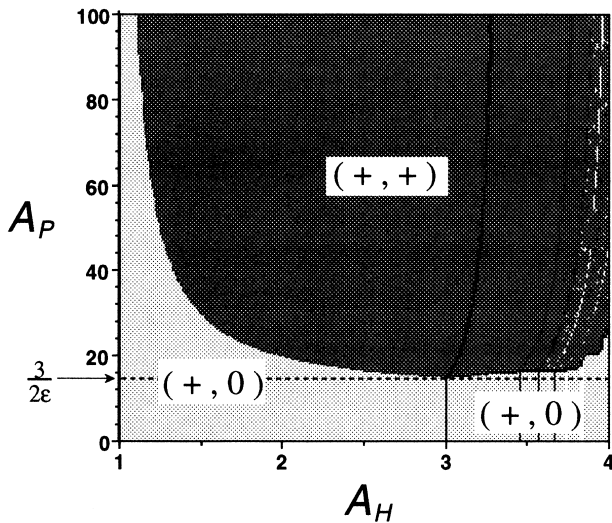


FIG. 15. (A_H, A_P) -dependence of the coexistence, obtained by numerical calculations. The region of $(+, 0)$ corresponds to where host persists while parasite goes extinct. The region of $(+, +)$ corresponds to coexistence of host and parasite. For $A_H < 1$, both parasite and host go extinct.

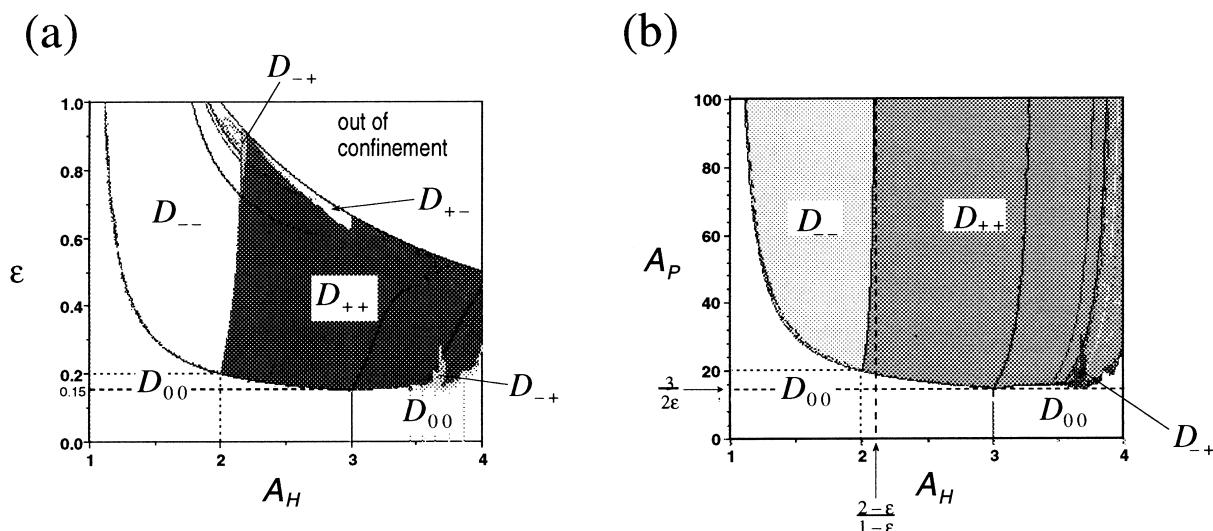


FIG. 16. Comparison of the mean and the lowest host population densities at the stationary state between when parasite and host coexist and when parasite is absent. D_{00} : both the mean and the lowest densities are coincides each other between two cases. D_{+-} : the mean is higher when they coexist than when parasite is absent, while the lowest when host and parasite coexist does not exceed that when parasite is absent. D_{-+} : the mean when they coexist does not exceed that when parasite is absent, while the lowest is higher when they coexist than when parasite is absent. D_{++} : both the mean and the lowest densities are higher when they coexist than when parasite is absent. (a) $H_0 = P_0 = 0.1$; $A_P = B_P = 10.0$; (b) $H_0 = P_0 = 0.1$; $\epsilon = 0.1$; $B_P = 0.15$.

This boundary curve (24) between D_{++} and D_{--} for equilibrium state (H^*, P^*) in Fig. 16 is connected to the point given by $A_H = 2$ and $\epsilon A_P = 2$, and the boundary (24) in Fig. 16(b) has the asymptote $A_H = (2 - \epsilon)/(1 - \epsilon)$ (Appendix D). For fixed ϵ , as shown in Fig. 16(b), if $A_H \geq (2 - \epsilon)/(1 - \epsilon)$, when parasite and host coexist, the lowest host population density is higher independently of parameter A_P , and the mean density is also higher for almost every parameter A_P . In contrast, if $A_H \leq 2$, coexistence results in some reduction of both the mean and the lowest densities, independently of both ϵ and A_P . If $2 < A_H < (2 - \epsilon)/(1 - \epsilon)$, the coexistence shifts up both the mean and the lowest densities only when host coexists with parasite with sufficiently small A_P , while the invasion success of parasite with sufficiently large A_P causes to shift them down.

From the characteristics of the boundary curve in Fig. 16, given by (24) and (25), we can prove that the parameter region D_{--} expands as A_P gets larger for fixed ϵ or as ϵ gets larger for fixed A_P (see Appendix D). Therefore, coexistence is more likely to be beneficial for the host from the viewpoint of population persistence if the coexisting parasite has smaller ϵ and/or smaller A_P .

4. Discussion

In this paper, we have analysed a mathematical model, described by a discrete dynamical system,

of host-parasite population dynamics for brood-parasitism with parasite-accepting host. The results indicate that some coexistence between parasite and host can be beneficial for the persistence of the host population from the viewpoint of population dynamics. In particular, we have examined the lowest host population density at the stationary state of the system. We consider that it would be more beneficial for the persistence of the host population if the lowest population density at the stationary state is higher, because the generation with the lower lowest density can be regarded as relatively more vulnerable to stochastic disturbance. This might cause drastic damage to the persistence of the host population.

Our results show that the parasite-accepting host population with the higher reproductive capacity, that is, with the larger A_H in our model, is more likely to benefit from coexistence with brood-parasite (see Fig. 16). There exists a threshold of the host quality, represented by the parameter A_H , beyond which coexistence is beneficial for host from the viewpoint of population persistence, if some parasite succeeds in invasion. In contrast, for a host with poorer quality, below the threshold, coexistence causes a reduction in host population persistence (see Fig. 16). In such a host-parasite system, the host population might become threatened with extinction because the lowest population density at the stationary state becomes lower due to coexistence with the brood-parasite.

In addition, coexistence with a brood-parasite that has a higher parasitization capacity, that is, a larger value of ϵA_p in our model, is more likely not to be beneficial for the host from the viewpoint of host population persistence. Since too low a parasitization capacity of parasite causes failure of invasion, only a parasite that has an intermediate parasitization capacity is likely to benefit the host from the viewpoint of host population persistence. In other words, the host-parasite system with such a *prudent* parasite could exist in a stationary state. This conclusion can be regarded as corresponding to the hypothesis about the stationary existence of brood-parasitism with parasite-accepting host, i.e. "Parasite is sufficiently prudent to avoid over-exploiting host population to extinction". Sufficiently large a value of ϵA_p could be regarded as corresponding to over-exploitation by the parasite.

Since decreasing the lowest density of host population at the stationary state causes reduction in host population persistence so that it is more likely to go extinct due to some ecological disturbance, we suggest that the host-parasite system with such a handicap would be ecologically unstable. Over a long period, such a host-parasite system might have gone extinct one by one, as a hypothesis about the stationary existence of brood-parasitism with parasite-accepting host says that "All other host-parasite systems are unstable and have already gone extinct, so that we can observe only stable ones". From this standpoint, it is expected that the existing stationary system with brood-parasite and parasite-accepting host would be likely to work to the benefit of the persistence of the host population. May & Robinson (1985) used mathematical models to discuss certain host populations that seemed threatened with extinction owing to parasitism. They focused on the stationary equilibrium state. Such host-parasite systems would correspond to those with the above-mentioned handicap. In our results, indicated in Fig. 16, the equilibrium state of the stationary coexistence contains D_{--} and D_{++} regions. The host-parasite coexisting system corresponding to D_{--} causes a lower equilibrium density of host population, which can be regarded as corresponding to the case discussed by May & Robinson (1985).

As for the existence of parasite-rejecting hosts—for example, the American robin *Turdus migratorius* and the grey catbird *Dumetella carolinensis* against the brood-parasitic cowbird (Rothstein, 1975a, b, 1982)—we can present a conjecture, from the viewpoint of population dynamical stability, that the coexistence of brood-parasite and parasite-accepting host corre-

sponding to cowbird might result in reduction of host population persistence. Such a system may be likely to become extinct due to some ecological disturbance. From this point, since our results show that this is the situation for a brood-parasite with high parasitization capacity (i.e. with a large value of ϵA_p), the persistent system with such a brood-parasite population might require a parasite-rejecting host population. This agrees with the observations for host-parasite relationships in birds, which show that the proportion of parasite-rejecting hosts increases with the parasitization rate, while that of parasite-acceptors increases as the parasitization rate decreases (Rothstein, 1975a, b, 1982). Further, since our results suggest that a parasite-accepting host population of poorer quality (i.e. with the smaller A_H) has its population persistence reduced by coexistence with the brood-parasite population, the coexistent system might become extinct due to some ecological disturbance, so that the persistent system with a poor-quality host population requires rejective behaviour by the host. In other words, for a poor-quality host population, only a system with a parasite-rejecting host can be ecologically stable and persist in a stationary state.

Note that the mean host population density at the stationary state also increases in almost all cases where parasite and host coexist and the lowest host population density increases, compared to when the parasite is absent. Conversely, the mean density decreases in almost all cases when the lowest density decreases and coexistence is disadvantageous from the viewpoint of host population persistence. This implies that ecologically stable (beneficial) coexistence can on average result in abundant host population, while ecologically unstable (non-beneficial) coexistence can reduce it, compared to when parasite is absent.

In our model, some assumptions would be unrealistic for host-parasite relations observed in nature. However, as mentioned in the section on modelling assumptions, for certain cases the assumptions are not necessarily unrealistic. For example, the case of the brood-parasitic mochokid catfish *Synodontis multipunctatus* in Lake Tanganyica. In particular, one of the assumptions, that of non-overlapping generations, is an oversimplification for the sake of mathematical simplicity. Indeed, one of the simple extensions of our model is to introduce the survival ratio of adult population to the next breeding season: σ_h for host and σ_p for brood-parasite. The model then has additional terms $\sigma_h h_n$ and $\sigma_p p_n$ on the right-hand sides of eqns (10) and (11). Some numerical calculations about such an extended model for the case when $\epsilon=0.1$ and $B_p=0.15$ give qualitatively the

same results as for non-overlapping generations. Other extensions of the mathematical model are possible, for example introducing age structure, age-dependent birth and death, multiple parasites, multi-species of hosts, and parasite-rejecting host.

In summary our results show the possible benefit, from a population dynamics viewpoint, to a host that might at first sight appear to be at a disadvantage by accepting the parasite.

The authors are indebted to Toshiyuki Ogawa, Kunimochi Sakamoto, Fugo Takasu, and anonymous referees for their valuable comments for carrying out and completing this work. The authors also thank Masayasu Mimura, Hiroyuki Matsuda and Katsuki Nakai for their encouragement.

REFERENCES

- BAKER, G. L. & GOLLUB, J. P. (1990). *Chaotic Dynamics: An Introduction*. Cambridge: Cambridge University Press.
- BEGON, M., HARPER, J. L. & TOWNSEND, C. R. (1990). *Ecology*, 2nd edn. Cambridge: Blackwell Scientific Publications.
- BROOK, M. DE L. & DAVIEW, N. B. (1988). Egg mimicry by cuckoos *Cuculus canorus* in relation to discrimination by hosts. *Nature* **335**, 630–632.
- DAWKINS, R. & KREBS, J. R. (1979). Arms races between and within species. *Proc. R. Soc. Lond. B* **205**, 489–511.
- DEVANEY, R. L. (1989). *An Introduction to Chaotic Dynamical Systems*, 2nd edn. California: Addison-Wesley.
- HÉNON, M. (1976). A two-dimensional mapping with a strange attractor. *Commun. Math. Phys.* **50**, 69–77.
- HÖLDOBLER, B. (1971). Communication between ants and their guests. *Sci. Am.* **224**, 86–93.
- KREBS, J. R. & DAVIES, N. B. (1987). *An Introduction to Behavioural Ecology*. Oxford: Blackwell.
- MAY, R. M. (1976). Simple mathematical models with very complicated dynamics. *Nature* **26**, 459–467.
- MAY, R. M. (1974). *Stability and Complexity in Model Ecosystems*. Princeton, NJ: Princeton University Press.
- MAY, R. M. & ROBINSON, S. K. (1985). Population dynamics of avian brood parasitism. *Am. Nat.* **126**, 475–494.
- NEE, S. & MAY, R. M. (1993). Population-level consequences of conspecific brood parasitism in birds and insects. *J. theor. Biol.* **161**, 95–109.
- ROTHSTEIN, S. I. (1975a). Evolutionary rates and host defences against avian brood parasitism. *Am. Nat.* **109**, 161–176.
- ROTHSTEIN, S. I. (1975b). An experimental and teleonomic investigation of avian brood parasitism. *Condor* **77**, 250–271.
- ROTHSTEIN, S. I. (1982). Mechanisms of avian egg recognition: which egg parameters elicit responses by rejector species? *Behav. Ecol. Sociobiol.* **11**, 229–239.
- SATO, T. (1986). A brood parasitic catfish of mouthbrooding cichlid fishes in Lake Tanganyika. *Nature* **323**, 58–59.
- SATO, T. (1988). Host preference of the brood parasitic catfish, *Synodontis multipunctatus*. In: *Ecological and Limnological Study on Lake Tanganyika and Adjacent Regions*, Vol. 5 (Kawanabe, H. & Kwetuenda, M. K., eds), pp. 25. Japan: Kyoto University.
- SLATKIN, M. & MAYNARD SMITH, J. (1979). Models of coevolution. *Q. Rev. Biol.* **54**, 233–263.
- TAKASU, F., KAWASAKI, K., NAKAMURA, H., COHEN, J. E. & SHIGESADA, N. (1993). Modeling the population dynamics of a cuckoo-host association and the evolution of host defenses. *Am. Nat.* **142**, 819–839.
- UTIDA, S. (1957). Cyclic fluctuations of population density intrinsic to the host-parasite system. *Ecology* **38**, 442–449.
- WIGGINS, S. (1990). *Introduction to Applied Nonlinear Dynamical Systems and Chaos*. New York: Springer-Verlag.

APPENDIX A

In this appendix we determine the confinement condition (19) in the main text for the non-negativeness of (H_n, P_n) according to the map corresponding to the system of eqns (17) and (18). With non-dimensionalized variables, when $P_n \equiv 0$, the system of (17) and (18) becomes one-dimensional:

$$H_{n+1} = A_H H_n (1 - H_n). \quad (\text{A.1})$$

The largest value of H_{n+1} is $A_H/4$ for $H_n = 1/2$. Hence, H_{n+1} satisfies the following for non-negative H_n not beyond 1 (see Fig. A1):

$$0 \leq H_{n+1} \leq \frac{A_H}{4}. \quad (\text{A.2})$$

This means that the map $H_n \mapsto H_{n+1}$ maps the interval $[0, 1]$ to $[0, A_H]$, as clearly shown in Fig. A1. If $A_H/4$ is larger than 1, H_{n+1} for H_n sufficiently near $1/2$ becomes > 1 , and H_{n+2} becomes negative by (A.1). On the other hand, if $A_H/4$ is not beyond 1, H_{n+1} is on $[0, 1]$ for any H_n of $[0, 1]$. Therefore, the confinement condition for the non-negativeness of H_n for any n and any initial value H_0 of $[0, 1]$ should be as follows:

$$\frac{A_H}{4} \leq 1. \quad (\text{A.3})$$

This is the well-known confinement condition for the discrete logistic dynamical system (A.1).

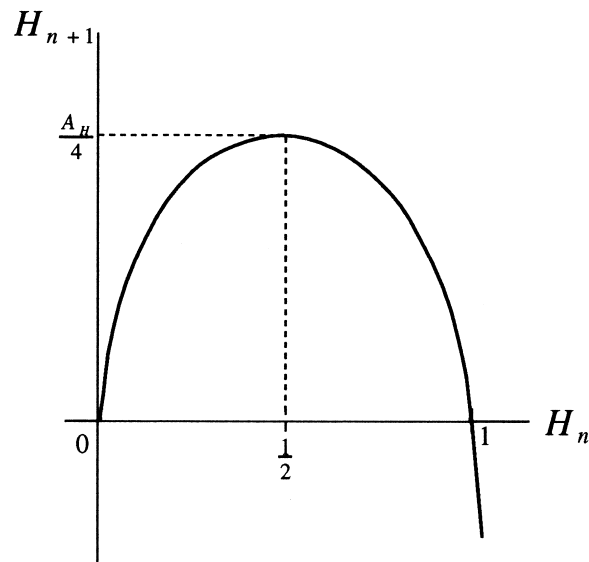


FIG. A1. Map $H_n \mapsto H_{n+1}$ corresponding to eqn (A.3).

As mentioned in the main text, the system of (17) and (18) is of logistic nature: the maps $H_n \mapsto H_{n+1}$ and $P_n \mapsto P_{n+1}$ are unimodal (see Fig. 3). By similar argument to (A.1), the necessary condition for the non-negativeness of H_n , corresponding to (A.3), is expressed as follows for the map corresponding to (17) [see Fig. 3(a)]:

$$\frac{A_H}{4} \leq \frac{1}{1 - \epsilon F(P_n)}. \tag{A.4}$$

Now, since the system (A.1) is of the particular case for the system of (17) and (18) with $P_n \rightarrow 0$, the system of (17) and (18) must satisfy the condition (A.3). Then, since the right-hand side of (A.4) is always ≥ 1 for any P_n , the condition (A.4) with (A.3) can be always satisfied for any $n \geq 1$ and any initial non-negative value P_0 . Therefore, by this argument, it is also shown that H_n of the system of (17) and (18) with (A.3) satisfies (A.2), that is, $H_n \in \mathbf{I} \equiv [0, A_H/4]$ for any $n \geq 1$.

In contrast, as for the map $P_n \mapsto P_{n+1}$ given by (18) according to positive P_n , the right-hand side of (18) is always positive not beyond $A_p/4B_p$ for $H_n \in \mathbf{J}_1 \equiv [0, 1/\epsilon B_p]$, because $0 < F(P_n) < 1$ for any non-negative P_n so that $\epsilon B_p F(P_n) H_n$ is less than 1 [see Fig. 3(c,d)]. For $H_n \in \mathbf{J}_2 \equiv (1/\epsilon B_p, +\infty)$, as indicated in Fig. 3(b), the condition for non-negativeness of P_{n+1} , corresponding to (A.3), can be expressed as follows:

$$\frac{A_p}{4B_p} \leq \frac{1}{\epsilon B_p H_n - 1},$$

that is,

$$H_n \leq \frac{1}{\epsilon} \left(\frac{4}{A_p} + \frac{1}{B_p} \right). \tag{A.5}$$

As $H_n \in \mathbf{I} \equiv [0, A_H/4]$ for any $n \geq 1$ as mentioned above, the condition (30) is required when $H_n \in \mathbf{I} \cap \mathbf{J}_2$. Now, H_n can be classified depending on which interval H_n is included in, $\mathbf{I}_1 \equiv \mathbf{I} \cap \mathbf{J}_1$ or $\mathbf{I}_2 \equiv \mathbf{I} \cap \mathbf{J}_2$. If $1/\epsilon B_p \geq A_H/4$, then $\mathbf{I}_2 = \emptyset$ and always $H_n \in \mathbf{I}_1$, while, if $1/\epsilon B_p < A_H/4$, $\mathbf{I}_2 \neq \emptyset$ and some H_n can be in $\mathbf{I}_2 = (1/\epsilon B_p, A_H/4]$. We note that (A.5) is satisfied when $1/\epsilon B_p \geq A_H/4$, provided (A.3), because H_n satisfies (A.2) and the right hand side of (A.5) is larger than $1/\epsilon B_p$. Non-negativeness of P_{n+1} is satisfied as long as $H_n \in \mathbf{I}_1$, while it could be violated without the condition (A.5) if $H_n \in \mathbf{I}_2$. Therefore, for the non-negativeness of P_n for any $n \geq 1$, it is now required that any $H_n \in \mathbf{I}_2$ satisfies the condition (A.5). Lastly, this argument brings condition (19).

APPENDIX B

From eqn (20) in the main text, we can easily drive the following equation:

$$\left(Q^* - \frac{1}{1-\epsilon} \right) (Q^* - A_H) \left\{ (Q^* - A_H)(Q^* - 1) + \frac{A_H}{B_p} \right\} = \frac{1}{1-\epsilon} \frac{A_H^2}{A_p B_p}, \tag{B.1}$$

where

$$Q^* \equiv \frac{1}{1 - \epsilon F(P^*)}. \tag{B.2}$$

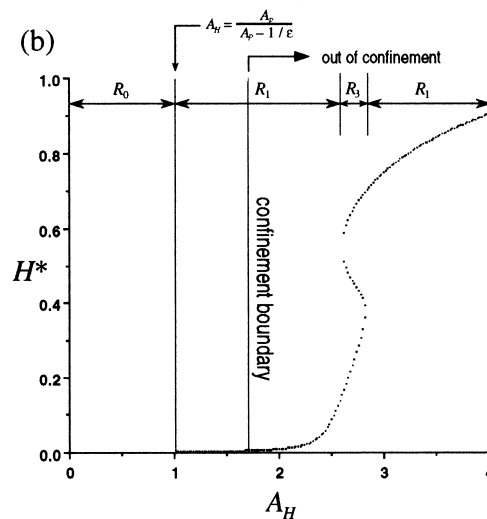
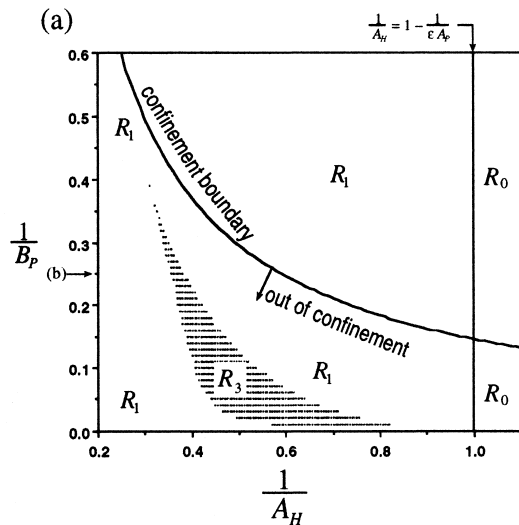


FIG. B1. (a) A numerical result for the (A_H, B_p) -dependence of the number of positive equilibrium states. $H_0 = P_0 = 0.1$; $\epsilon = 0.6$; $A_p = 1000.0$. R_0 : no positive equilibrium exists. R_1 : only one positive equilibrium exists. R_3 : three different positive equilibria coexist for each (A_H, A_p) . R_3 is out of the confinement condition (19). (b) Numerical plots of the positive equilibria for a variety of A_H . $H_0 = P_0 = 0.1$; $\epsilon = 0.6$; $A_p = 1000.0$; $B_p = 4.0$.

From definition (B.2), since $0 < F(P^*) < 1$ for any positive P^* , the meaningful root Q^* for (B.1) should be in the following range:

$$1 < Q^* < \frac{1}{1-\epsilon}. \quad (\text{B.3})$$

The number of roots Q^* for (B.1) with (B.3) is equivalent to that of positive solutions (H^*, P^*) for (20). Without the confinement condition (19), the number of solutions could be more than one (see Fig. B1). However, under the confinement condition (19), only one meaningful root $Q^* > 1$ for (B.1), that is, only one positive solution (H^*, P^*) for (20) can be found by numerical calculations.

APPENDIX C

In this appendix, we analyse the local stability of the equilibrium state: Case 1 when $(H^*, P^*) = (0, 0)$; Case 2 when $(H^*, P^*) = (+, 0)$. For Case 3 when $(H^*, P^*) = (+, +)$, since the equilibrium state cannot be obtained in any practical form, we examined the stability only by numerical calculations.

By linearizing the system of (17) and (18), we get the following linear dynamical system for the perturbation (η_n, π_n) around the equilibrium (H^*, P^*) :

$$\begin{pmatrix} \eta_{n+1} \\ \pi_{n+1} \end{pmatrix} = M \begin{pmatrix} \eta_n \\ \pi_n \end{pmatrix}, \quad (\text{C.1})$$

where

$$M = \begin{pmatrix} m_{11} & m_{12} \\ m_{21} & m_{22} \end{pmatrix} \quad (\text{C.2})$$

$$m_{11} = A_H [1 - \epsilon F(P^*)] \{1 - 2[1 - \epsilon F(P^*)]H^*\}$$

$$m_{12} = -\epsilon A_H \{1 - 2[1 - \epsilon F(P^*)]H^*\} \frac{dF(P^*)}{dP^*}$$

$$m_{21} = \epsilon A_P H^* (1 - 2\epsilon B_P F(P^*) H^*) F(P^*)$$

$$m_{22} = \epsilon A_P H^* (1 - 2\epsilon B_P F(P^*) H^*) \frac{dF(P^*)}{dP^*}.$$

Local stability of the equilibrium state depends on the eigenvalues of the matrix M given by (C.2): If and only if any eigenvalue for M has an absolute value of < 1 , the local stability is established for (H^*, P^*) (for instance, see May, 1974).

In Case 1, eigenvalues of the matrix M are A_H and 0. Therefore, the condition that the absolute value of any eigenvalue is < 1 , that is, for local stability, is given by eqn (22) in the main text.

In Case 2, eigenvalues of matrix M are $A_H(1 - 2H^*)$ and $\epsilon A_P H^*$. Thus, the condition for local stability is as follows:

$$\begin{cases} -1 < A_H(1 - 2H^*) < 1 \\ 0 < \epsilon A_P H^* < 1. \end{cases}$$

Since $H^* = 1 - 1/A_H > 0$ from eqn (21), lastly, the condition for local stability for Case 2 becomes eqn (23) in the main text.

APPENDIX D

In this appendix, the boundary between D_{++} and D_{--} within the parameter region for the equilibrium state (H^*, P^*) in Fig. 16 can be analytically derived. As long as the equilibrium state is considered, since both the mean and the lowest values of equilibrium H^* are identical to the value of H^* itself, and since the difference between the cases where parasite and host coexist and where the parasite is absent should be zero on the considered boundary, H^* on the boundary is given by (21) which gives the equilibrium when the parasite is absent. Then, from the first equation of (20), we obtain the equilibrium P^* on the boundary as follows:

$$P^* = \frac{1}{1-\epsilon} \cdot \frac{A_H - 2}{\frac{2-\epsilon}{1-\epsilon} - A_H}, \quad (\text{D.1})$$

which is non-negative only when (25) is satisfied. Substituting (21) and (D.1) into the second equation of (20), we get the relation (24) among parameters.

The right-hand side of (24) becomes 2 for $A_H = 2$, independent of ϵ and B_P , which is the same parameter relation as the local stability boundary given by (23) for $A_H = 2$. Thus, since the boundary between D_{--} and D_{00} coincides with the local stability boundary given by (23), the critical boundaries among D_{--} , D_{++} , and D_{00} meet at the point corresponding to $(A_H, \epsilon A_P) = (2, 2)$ (see Fig. 16). The critical point $(A_H, \epsilon) = (2, 2/A_P)$ in Fig. 16(a) decreases as A_P gets larger, and $(A_H, A_P) = (2, 2/\epsilon)$ in Fig. 16(b) decreases as ϵ gets larger. Further, since the derivative $\partial\epsilon/\partial A_P$ in terms of the boundary curve given by (24) is negative under the condition (25), the boundary curve monotonically shifts down as A_P gets larger [Fig. 16(a)], and as ϵ gets larger [Fig. 16(b)]. It is easily shown that the right-hand side of (24) $\rightarrow +\infty$ as $A_H \rightarrow (2-\epsilon)/(1-\epsilon)$ from below, so that the boundary curve in Fig. 16(b) has asymptote $A_H = (2-\epsilon)/(1-\epsilon)$, which is monotonically increasing as ϵ gets larger. These characteristics of the boundary curve between D_{++} and D_{--} for the equilibrium state (H^*, P^*) in Fig. 16 means that the parameter region D_{--} expands as A_P gets larger for fixed ϵ or as ϵ gets larger for fixed A_P .